

H. G. Cunningham

Rep. 835 - R. T. Jones

**NATIONAL ADVISORY COMMITTEE
FOR AERONAUTICS**

REPORT No. 835

**PROPERTIES OF LOW-ASPECT-RATIO POINTED WINGS
AT SPEEDS BELOW AND ABOVE THE SPEED
OF SOUND**

By ROBERT T. JONES



1946

AERONAUTIC SYMBOLS 1. FUNDAMENTAL AND DERIVED UNITS

	Symbol	Metric		English	
		Unit	Abbrevia- tion	Unit	Abbrevia- tion
Length	l	meter	m	foot (or mile)	ft (or mi)
Time	t	second	s	second (or hour)	sec (or hr)
Force	F	weight of 1 kilogram	kg	weight of 1 pound	lb
Power	P	horsepower (metric)		horsepower	hp
Speed	V	{ kilometers per hour { meters per second	kph mps	miles per hour feet per second	mph fps

2. GENERAL SYMBOLS

W	Weight = mg	ν	Kinematic viscosity
g	Standard acceleration of gravity = 9.80665 m/s ² or 32.1740 ft/sec ²	ρ	Density (mass per unit volume)
m	Mass = $\frac{W}{g}$		Standard density of dry air, 0.12497 kg-m ⁻³ at 15° C and 760 mm; or 0.002378 lb-ft ⁻³ sec ²
I	Moment of inertia = mk^2 . (Indicate axis of radius of gyration k by proper subscript.)		Specific weight of "standard" air, 1.2255 kg/m ³ or 0.07651 lb/cu ft
μ	Coefficient of viscosity		

3. AERODYNAMIC SYMBOLS

S	Area	i_w	Angle of setting of wings (relative to thrust line)
S_w	Area of wing	i_s	Angle of stabilizer setting (relative to thrust line)
G	Gap	Q	Resultant moment
b	Span	Ω	Resultant angular velocity
c	Chord	R	Reynolds number, $\rho \frac{Vl}{\mu}$ where l is a linear dimen- sion (e.g., for an airfoil of 1.0 ft chord, 100 mph, standard pressure at 15° C, the corresponding Reynolds number is 935,400; or for an airfoil of 1.0 m chord, 100 mps, the corresponding Reynolds number is 6,865,000)
A	Aspect ratio, $\frac{b^2}{S}$	α	Angle of attack
V	True air speed	ϵ	Angle of downwash
q	Dynamic pressure, $\frac{1}{2}\rho V^2$	α_o	Angle of attack, infinite aspect ratio
L	Lift, absolute coefficient $C_L = \frac{L}{qS}$	α_i	Angle of attack, induced
D	Drag, absolute coefficient $C_D = \frac{D}{qS}$	α_a	Angle of attack, absolute (measured from zero- lift position)
D_o	Profile drag, absolute coefficient $C_{D_o} = \frac{D_o}{qS}$	γ	Flight-path angle
D_i	Induced drag, absolute coefficient $C_{D_i} = \frac{D_i}{qS}$		
D_p	Parasite drag, absolute coefficient $C_{D_p} = \frac{D_p}{qS}$		
C	Cross-wind force, absolute coefficient $C_c = \frac{C}{qS}$		

NACA-TR 835

REPORT No. 835

**PROPERTIES OF LOW-ASPECT-RATIO POINTED WINGS
AT SPEEDS BELOW AND ABOVE THE SPEED
OF SOUND**

By ROBERT T. JONES

**Langley Memorial Aeronautical Laboratory
Langley Field, Va.**

National Advisory Committee for Aeronautics

Headquarters, 1500 New Hampshire Avenue NW, Washington 25, D. C.

Created by act of Congress approved March 3, 1915, for the supervision and direction of the scientific study of the problems of flight (U. S. Code, title 49, sec. 241). Its membership was increased to 15 by act approved March 2, 1929. The members are appointed by the President, and serve as such without compensation.

JEROME C. HUNSAKER, Sc. D., Cambridge, Mass., *Chairman*

THEODORE P. WRIGHT, Sc. D., Administrator of Civil Aeronautics, Department of Commerce, *Vice Chairman*.

Hon. WILLIAM A. M. BURDEN, Assistant Secretary of Commerce.

VANNEVAR BUSH, Sc. D., Chairman, Joint Research and Development Board.

EDWARD U. CONDON, Ph. D., Director, National Bureau of Standards.

R. M. HAZEN, B. S., Chief Engineer, Allison Division, General Motors Corp.

WILLIAM LITTLEWOOD, M. E., Vice President, Engineering, American Airlines System.

EDWARD M. POWERS, Major General, United States Army, Assistant Chief of Air Staff-4, Army Air Forces, War Department.

ARTHUR W. RADFORD, Vice Admiral, United States Navy, Deputy Chief of Naval Operations (Air), Navy Department.

ARTHUR E. RAYMOND, M. S., Vice President, Engineering, Douglas Aircraft Co.

FRANCIS W. REICHELDERFER, Sc. D., Chief, United States Weather Bureau.

LESLIE C. STEVENS, Rear Admiral, United States Navy, Bureau of Aeronautics, Navy Department.

CARL SPAATZ, General, United States Army, Commanding General, Army Air Forces, War Department.

ALEXANDER WETMORE, Sc. D., Secretary, Smithsonian Institution.

ORVILLE WRIGHT, Sc. D., Dayton, Ohio.

GEORGE W. LEWIS, Sc. D., *Director of Aeronautical Research*

JOHN F. VICTORY, LL.M., Executive Secretary

HENRY J. E. REID, Sc. D., Engineer-in-charge, Langley Memorial Aeronautical Laboratory, Langley Field, Va.

SMITH J. DEFRANCE, B. S., Engineer-in-charge, Ames Aeronautical Laboratory, Moffett Field, Calif.

EDWARD R. SHARP, LL. B., Manager, Aircraft Engine Research Laboratory, Cleveland Airport, Cleveland, Ohio

CARLTON KEMPER, B. S., Executive Engineer, Aircraft Engine Research Laboratory, Cleveland Airport, Cleveland, Ohio

TECHNICAL COMMITTEES

AERODYNAMICS
POWER PLANTS FOR AIRCRAFT
AIRCRAFT CONSTRUCTION
OPERATING PROBLEMS

MATERIALS RESEARCH COORDINATION
SELF-PROPELLED GUIDED MISSILES
SURPLUS AIRCRAFT RESEARCH
INDUSTRY CONSULTING COMMITTEE

Coordination of Research Needs of Military and Civil Aviation

Preparation of Research Programs

Allocation of Problems

Prevention of Duplication

Consideration of Inventions

LANGLEY MEMORIAL AERONAUTICAL LABORATORY,
Langley Field, Va.

AIRCRAFT ENGINE RESEARCH LABORATORY, Cleveland Airport, Cleveland, Ohio

Conduct, under unified control, for all agencies, of scientific research on the fundamental problems of flight

AMES AERONAUTICAL LABORATORY,
Moffett Field, Calif.

OFFICE OF AERONAUTICAL INTELLIGENCE, Washington, D. C.

Collection, classification, compilation, and dissemination of scientific and technical information on aeronautics

PROPERTIES OF LOW-ASPECT-RATIO POINTED WINGS AT SPEEDS BELOW AND ABOVE THE SPEED OF SOUND

BY ROBERT T. JONES

SUMMARY

Low-aspect-ratio wings having pointed plan forms are treated on the assumption that the flow potentials in planes at right angles to the long axis of the airfoils are similar to the corresponding two-dimensional potentials. For the limiting case of small angles of attack and low aspect ratios the theory brings out the following significant properties:

- (1) *The lift of a slender pointed airfoil moving in the direction of its long axis depends on the increase in width of the sections in a downstream direction. Sections behind the section of maximum width develop no lift.*
 - (2) *The spanwise loading of such an airfoil is independent of the plan form and approaches the distribution giving a minimum induced drag.*
 - (3) *The lift distribution of a pointed airfoil traveling point-foremost is relatively unaffected by the compressibility of the air below or above the speed of sound.*
- A test of a triangular airfoil at a Mach number of 1.75 verified the theoretical values of lift and center of pressure.*

INTRODUCTION

The assumption of small disturbances in a two-dimensional potential flow leads to the well-known thin-airfoil theory of Munk (reference 1) and the Prandtl-Glauert rule (references 2 and 3) at speeds less than sonic. At speeds above the speed of sound, application of the same assumptions leads to the Ackeret theory (reference 4) according to which the wing sections generate plane sound waves of small amplitude. As is well known, the Ackeret theory predicts a radical change in the properties of such wings on transition to supersonic velocities and these changes have been verified by experiments in supersonic wind tunnels (reference 5).

Both the Ackeret theory and the Munk theory apply to the case of a wing having a large span and a small chord. The present discussion is based on assumptions similar to those used by Ackeret and Munk but covers the opposite extreme, namely, the wing of small span and large chord. In the latter case the flow is expected to be two dimensional when viewed in planes perpendicular to the direction of motion.

A theory for the rectangular wing of small aspect ratio has been given by Bollay (reference 6). Bollay assumes a separated, or discontinuous, potential flow similar to the well-known Kirchhoff flow and shows that under these circumstances the lift is proportional to the square of the angle of attack. Bollay does not consider the effect of compressibility. The present treatment covers other plan forms and, although based on different assumptions, is not

inconsistent with Bollay's theory in the limiting case of small angles of attack.

By limiting the plan forms to small vertex angles, the properties of the wings in compressible flow at high subsonic and at supersonic speeds are also covered. Tsien (reference 7) has pointed out that Munk's airship theory (reference 8) applies to a slender body of revolution at speeds greater than sonic. The lift and moment of such a body are not expected to change appreciably with Mach number. The present paper gives an analysis of the low-aspect-ratio airfoil based on similar assumptions and shows that little change of the lift distribution of an airfoil of pointed plan form near the center of the Mach cone is to be expected.

SYMBOLS

V	flight velocity
α	angle of attack
S	wing area
A	aspect ratio $\left(\frac{b_{max}^2}{S}\right)$
x	distance along axis of symmetry of pointed airfoil measured downstream from nose
y	spanwise distance, measured from axis of symmetry
z	vertical distance from plane of wing
t	time
m'	additional apparent mass (spanwise section)
b	local span
c	chord
ρ	density of air
q	dynamic pressure $\left(\frac{1}{2}\rho V^2\right)$
l	local lift force (per length dx)
c_l	local lift coefficient $\left(\frac{l}{qb dx}\right)$
D_i	induced drag
C_{D_i}	induced-drag coefficient $\left(\frac{D_i}{qS}\right)$
L	total lift
C_L	lift coefficient $\left(\frac{L}{qS}\right)$
ϕ	surface potential
θ	spanwise-location parameter $\left(\cos^{-1}\frac{y}{b/2}\right)$
Δp	local pressure difference
M	Mach number, ratio of flight velocity to speed of sound
$x_{c.p.}$	distance of center of pressure from nose of airfoil
C_m	pitching-moment coefficient $\left(\frac{\text{Pitching moment}}{qSc_{max}}\right)$
L_M	lift at Mach number M
L_0	lift at zero Mach number
m_{max}	maximum (used as subscript)

THEORY FOR WINGS OF LOW ASPECT RATIO

The flow about an airfoil of very low aspect ratio may be considered two dimensional when viewed in cross sections perpendicular to the longitudinal axis. With this idealization, the treatment of the low-aspect-ratio airfoil becomes exceedingly simple; formulas are obtained that are similar in some respects to those derived by Munk (reference 8) and Tsien (reference 7) for an elongated body of revolution.

Perhaps the simplest case from the analytical point of view is that of the long, flat, triangular airfoil traveling point-foremost at a small angle of attack. Viewed from a reference system at rest in the undisturbed fluid, the flow pattern in a plane cutting the airfoil at a distance x from the nose is the familiar two-dimensional flow caused by a flat plate having the normal velocity $V\alpha$. (See fig. 1.) Observed in this plane, the width of the plate and hence the scale of the flow pattern continually increase as the airfoil progresses through the plane. This increase in the scale of the flow pattern requires a local lift force l equal to the downward velocity $V\alpha$ times the local rate of increase of the additional apparent mass m' , or

$$\begin{aligned} l &= V\alpha \frac{dm'}{dt} \\ &= V^2\alpha \frac{dm'}{dx} \\ V &= \frac{dx}{dt} \end{aligned}$$

since

By a well-known formula from two-dimensional-flow theory,

$$m' = \pi \frac{b^2}{4} \rho \frac{dx}{dt}$$

where b is the local width of the plate. Hence

$$\frac{dm'}{dx} = \pi \frac{b}{2} \rho \frac{db}{dx} \frac{dx}{dt}$$

and the lift l per length dx will be given by the expression

$$l = \pi\alpha \frac{\rho}{2} V^2 b \frac{db}{dx} dx$$

Dividing by $\frac{\rho}{2} V^2$ and by the area $b dx$ gives the local lift coefficient

$$c_l = \pi\alpha \frac{db}{dx} \quad (1)$$

When this flow is considered in more detail, it is found from the two-dimensional theory that the surface potential ϕ is distributed spanwise according to the ordinates of an ellipse, that is,

$$\begin{aligned} \phi &= \pm V\alpha \sqrt{\left(\frac{b}{2}\right)^2 - y^2} \\ &= \pm V\alpha \frac{b}{2} \sin \theta \end{aligned} \quad (2)$$

where $\cos \theta = \frac{y}{b/2}$ and the sign changes in going from the

upper to the lower surface of the airfoil. (See fig. 2.) An instant later, in the same plane, the ordinates are those of a slightly larger ellipse, corresponding to an increase of ϕ . The local pressure difference is given by the local rate of increase of ϕ , that is,

$$\begin{aligned} \Delta p &= 2\rho \frac{\partial \phi}{\partial t} \\ &= 2\rho V \frac{\partial \phi}{\partial x} \\ &= 2\rho V \frac{\partial \phi}{\partial b} \frac{db}{dx} \end{aligned} \quad (3)$$

where $\partial \phi / \partial b$ is a function of y . Differentiation of ϕ yields the equation

$$\begin{aligned} \Delta p &= 2\rho V^2 \frac{b}{\sqrt{\left(\frac{b}{2}\right)^2 - y^2}} \frac{db}{dx} \alpha \\ \text{or} \quad \frac{\Delta p}{q} &= \frac{2\alpha}{\sin \theta} \frac{db}{dx} \end{aligned} \quad (4)$$

The pressure distribution thus shows an infinite peak along the sloping sides of the airfoil similar to the pressure peak at the leading edge of a conventional airfoil. The distribution along radial lines passing through the vertex of the triangle (lines of constant $\frac{y}{b/2}$) is uniform (fig. 3), however, and the center of pressure coincides with the center of area.

Equations (1) and (4) show that the development of lift by the long slender airfoil depends on an expansion of the sections in a downstream direction; hence a part of the surface having parallel sides would develop no lift. Furthermore, a decreasing width would develop no lift. Further, require negative lift with infinite negative pressure peaks along the edges of the narrower sections. In the actual flow, however, the edge behind the maximum cross section will lie in the viscous or turbulent wake formed over the surface ahead; and for this reason it will be assumed that the infinite pressure difference indicated by equation (3) cannot be developed across these edges. It is this assumption, corresponding to the Kutta condition, which gives the plate the properties of an airfoil as distinct from another type of body, such as a body of revolution.

V

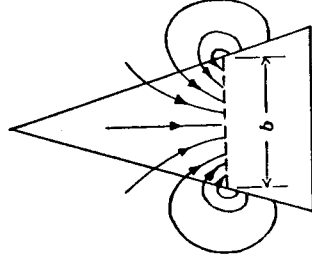


FIGURE 1.—Flow pattern.

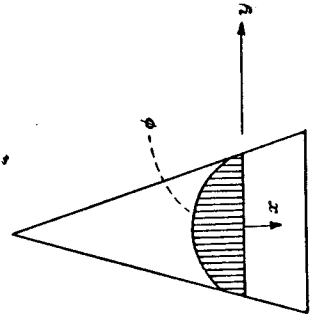


FIGURE 2.—Potential.

With the aid of the Kutta condition, it may easily be shown that sections of the airfoil behind the section of greatest width develop no lift. A potential flow satisfying both the boundary condition and the Kutta condition may be obtained by the introduction of a free surface of discontinuity behind the widest section. This surface of discontinuity (fig. 4) would be composed of parallel vortices extending downstream from the widest section of the airfoil as prolongations of the vortices representing the discontinuity of potential over the forward part of the airfoil. This sheet, although possibly wider than the downstream sections of the airfoil, still satisfies their boundary condition, since the lateral arrangement of the vortices is such as to give uniform downward velocity equal to $V\alpha$ over the entire width of the sheet including the rearward portion of the airfoil. Since the pressure difference across the airfoil is proportional to $\partial\phi/\partial x$ and since this gradient disappears as soon as the vortices become parallel to the stream, no lift is developed on the rearward sections.

Integration of the pressures in a chordwise direction from the leading edge downstream to the widest section will give the span load distribution and the induced drag. The span load distribution is

$$\frac{\partial L}{\partial y} = \int \Delta p dx$$

or, from equation (3),

$$\frac{\partial L}{\partial y} = 2\rho V\phi$$

From equation (2),

$$\phi = V\alpha \frac{b_{max}}{2} \sin \theta$$

Hence $\partial L/\partial y$ is elliptical and independent of the plan form. With the elliptical span load the induced drag is a minimum and is equal to

$$D_i = \frac{L^2}{\pi q b_{max}^2} \quad (5)$$

A second integration of $\frac{\partial L}{\partial y} dy$ across the widest section gives the total lift, which is

$$L = \frac{\pi}{4} \rho V^2 \alpha b_{max}^2 \quad (6)$$

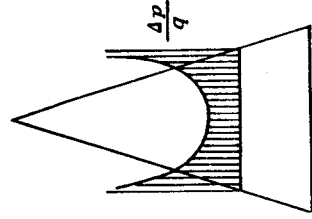


FIGURE 3.—Pressure distribution.

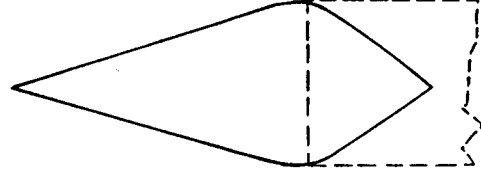


FIGURE 4.—Wake.

The lift of the slender airfoil therefore depends only on the width and not on the area. If the lift is divided by $\frac{1}{2}\rho V^2 S$ and if the aspect ratio A is considered to be $\frac{b_{max}^2}{S}$, then

$$C_L = \frac{\pi}{2} A\alpha \quad (7)$$

and the induced-drag/coefficient is

$$C_{D_i} = \frac{C_L^2}{\pi A} = C_{D_i}^\alpha \quad (8)$$

From equation (8) it appears that the resultant force lies halfway between the normal to the surface and the normal to the air stream.

It is seen that in the case of a rectangular plan form the simplified formula (equation (4)) gives an infinite concentration of lift at the leading edge and no lift elsewhere, whereas a more accurate theory would show some distribution of the lift rearward. If the rate of increase of the width becomes too great, the flow cannot be expected to remain two dimensional. It can be shown by examination of the known three-dimensional (nonlifting) potential flow around an elliptic disk (reference 9), however, that the two-dimensional theory gives a good approximation in the case of an elliptical leading edge, which indicates that the theory

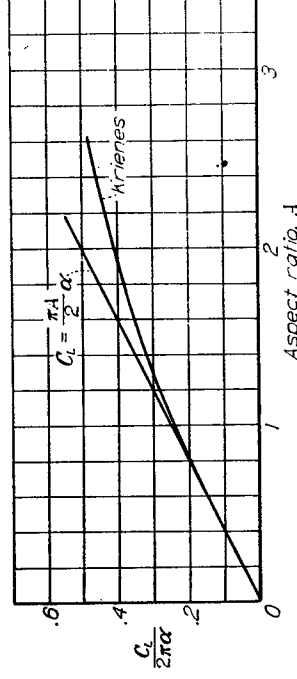


FIGURE 5.—Comparison of lift calculated by present theory for elliptical wings of low aspect ratio with results of Krienes (reference 10).

is applicable over a large range of nose shapes. In figure 5 is shown a comparison of the lift calculated by the present theory for elliptical wings of low aspect ratio with the results of the more accurate three-dimensional potential-flow calculations of Krienes (reference 10). The results are in good agreement up to aspect ratios approaching 1. Application of equation (4) gives a center of pressure on the elliptical plan form at one-sixth of the chord. Figure 6 also shows this value compared with values given by Krienes' theory. In this respect it appears that the agreement is not so good as for the lift.

EFFECT OF COMPRESSIBILITY

In order to show the effect of compressibility, use will be made of the theory of potential flow with small disturbances. Glauert (reference 2) and Prandtl (reference 3) have demonstrated that, at subsonic speeds, a distribution of potential satisfying Laplace's equation will satisfy the linearized compressible-flow equation if the distribution $\phi(x, y, z)$ is

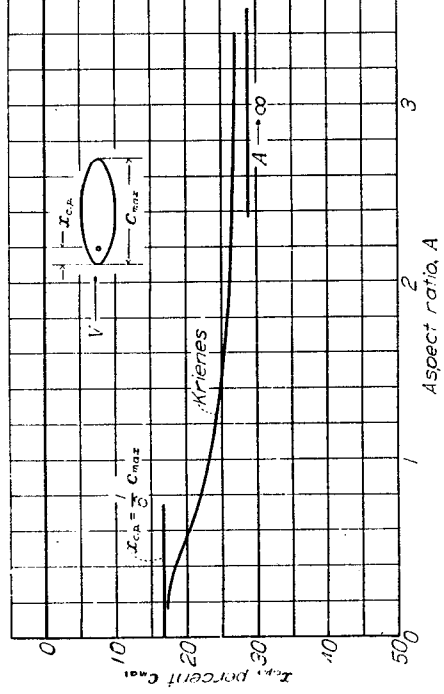


FIGURE 6.—Comparison of center of pressure calculated by present theory for elliptical wings of low aspect ratio with results of Krienes (reference 10).

foreshortened along the direction of motion by the transformation

$$x' = \frac{x}{\sqrt{1-M^2}} \quad y' = y \quad z' = z$$

This fact may be applied in a calculation procedure by starting with a fictitious airfoil longer in the x -direction than the true one and calculating the potential distribution for this airfoil by methods of incompressible flow. The correct dimensions and correct distribution of ϕ are then obtained when the transformation is applied.

For the long slender airfoil, the potential distribution at each section is similar to that for an infinitely long body; therefore $\partial\phi/\partial z$ and hence the local pressures vary in inverse proportion to the length. The foregoing calculation procedure gives a null result in this case, since the pressures calculated for the fictitious airfoil at $M=0$ will be reduced in the same ratio that the length is increased and the Lorentz transformation to restore the correct length will also restore the same pressures as those obtained at $M=0$. Since $\partial\phi/\partial z$ is unchanged by the transformation, the normal velocity component and hence the angle of attack are unchanged also. These results can be obtained by referring directly to the linearized equation for the potential

$$(1-M^2) \frac{\partial^2\phi}{\partial x^2} + \frac{\partial^2\phi}{\partial y^2} + \frac{\partial^2\phi}{\partial z^2} = 0 \quad (9)$$

(See reference 3.) If the airfoil is sufficiently slender, $\partial^2\phi/\partial z^2$ can be neglected in comparison with $\partial\phi/\partial x$ except near the edge. Since the lift is proportional to $\partial\phi/\partial x$, the increase of the lift with Mach number can therefore be neglected in comparison with the lift.

It is important to note that the theory of small disturbances is not limited to subsonic velocities and that, so long as the term $(1-M^2) \frac{\partial^2\phi}{\partial x^2}$ in equation (9) remains small, the solution in the region of the wing will continue to be given by the potential (equation (2)). Evidently the Mach number cannot be increased indefinitely, for then the coefficient of $\partial^2\phi/\partial x^2$ will become so large that the first term will no longer be negligible. The required condition will be satisfied, however, by adopting a pointed plan form with the vertex angle so small that the entire surface lies near the center of the

Mach cone (fig. 7). The condition of a small vertex angle also necessary in order that the potential distribution equation (2) may apply. In the case of a wing with a blunt leading-edge plan form, abrupt changes in the flow arise transition to supersonic velocities, and potential flow of the subsonic type no longer exists.

The lift and lift distribution for rectangular surfaces supersonic speeds have been calculated by Schlichting (reference 11). Figure 7 shows the variation of lift-curve slope with Mach number as obtained from Schlichting's results for rectangular wings of two different aspect ratios and for a range of speeds in which the two Mach cones from the tip do not reach the center of the wing. In the subsonic range values given by the Prandtl-Glauert rule are shown. The curves are compared with the values indicated by the present theory for a triangular wing lying near the center of the Mach cone. Figure 8 shows the travel of the center of pressure for these plan forms. It is to be noted that, with blunt-leading-edge plan forms, the center of pressure travels from a point near the quarter chord to a point near the mid-chord when the velocity is increased above the speed of sound.

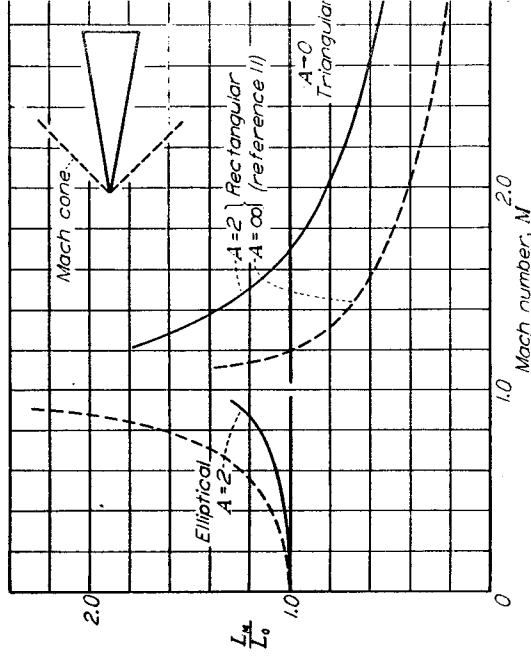


FIGURE 7.—Variation of lift with Mach number for different plan forms.

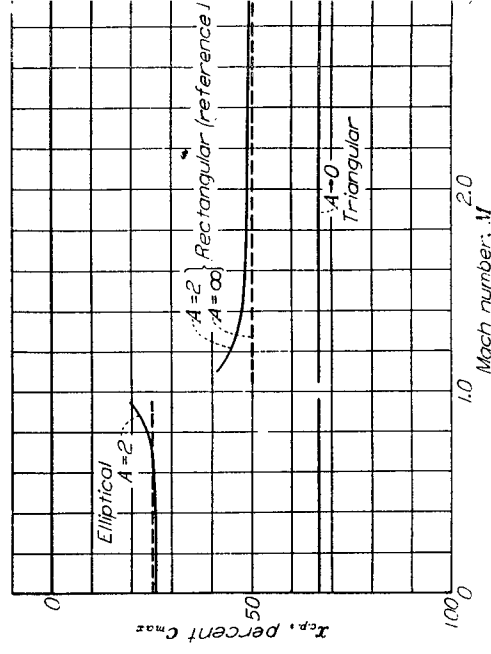


FIGURE 8.—Travel of center of pressure with Mach number for different plan forms.

TESTS OF A TRIANGULAR AIRFOIL AT SUPERSONIC SPEED

As a test of the foregoing analysis, a small triangular airfoil in the form of a steel plate with rounded leading edges was constructed and tested in the Langley model supersonic tunnel. The tests were made at a Mach number of 1.75. Figure 9 shows the details of the model and figure 10 summarizes the results of the test. At zero angle of attack a small lift and a small pitching moment occur, which are presumably the result of the camber given the airfoil by rounding off the leading edges in the manner shown by section A-A in figure 9. In general, the results are in good agreement with the theory if an allowance is made for this camber, as shown in figure 10.

CONCLUSIONS

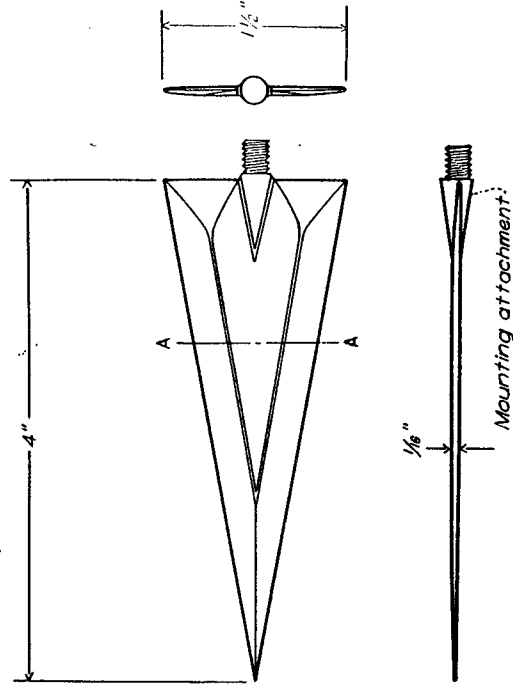
1. The lift of a slender, pointed airfoil moving in the direction of its long axis depends on the increase in width of the sections in a downstream direction. Sections behind the section of maximum width develop no lift.
2. The spanwise loading of such an airfoil is independent of the plan form and approaches the distribution giving a minimum induced drag.
3. The lift distribution of a pointed airfoil traveling point-foremost is relatively unaffected by the compressibility of the air below or above the speed of sound.

LANGLEY MEMORIAL AERONAUTICAL LABORATORY,
 NATIONAL ADVISORY COMMITTEE FOR AERONAUTICS,
 LANGLEY FIELD, VA., May 11, 1945.

REFERENCES

1. Munk, Max M.: Elements of the Wing Section Theory and of the Wing Theory. NACA Rep. No. 191, 1924.
2. Clauert, H.: The Effect of Compressibility on the Lift of an Airfoil. R. & M. No. 1135, British A. R. C., 1927.
3. Prandtl, L.: General Considerations on the Flow of Compressible Fluids. NACA TM No. 805, 1936.
4. Ackeret, J.: Air Forces on Airfoils Moving Faster Than Sound. NACA TM No. 317, 1925.
5. Taylor, G. I.: Applications to Aeronomics of Ackeret's Theory of Aerofoils Moving at Speeds Greater Than That of Sound. R. & M. No. 1467, British A. R. C., 1932.
6. Bollay, William: A Theory for Rectangular Wings of Small Aspect Ratio. Jour. Aero. Sci., vol. 4, no. 7, May 1937, pp. 294-296.
7. Tsien, Hsue-Shen: Supersonic Flow over an Inclined Body of Revolution. Jour. Aero. Sci., vol. 5, no. 12, Oct. 1938, pp. 480-483.

8. Munk, Max M.: The Aerodynamic Forces on Airship Hulls. NACA Rep. No. 184, 1924.
9. Lamb, Horace: Hydrodynamics. Sixth ed., Cambridge Univ. Press, 1932, pp. 146-153.
10. Krienes, Klaus: The Elliptic Wing Based on the Potential Theory. NACA TM No. 971, 1941.
11. Schlichting, H.: Airfoil Theory at Supersonic Speed. NACA TM No. 897, 1939.



Section A-A

Figure 9.—Airfoil tested in Langley model supersonic tunnel.

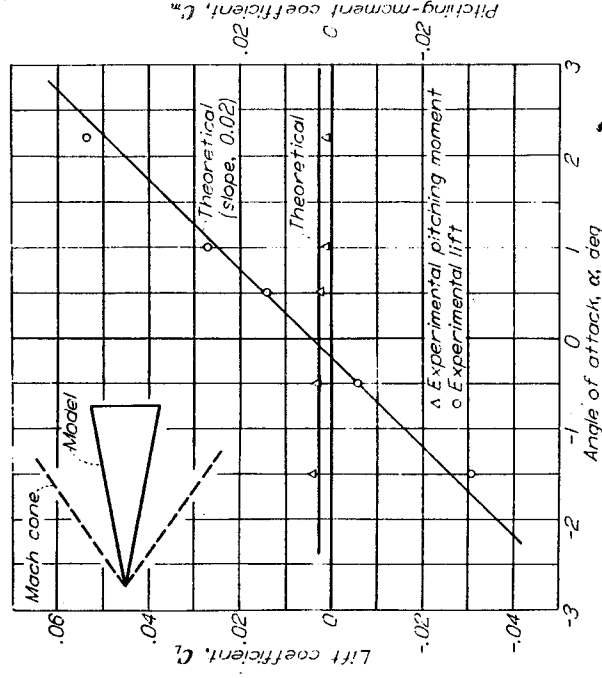
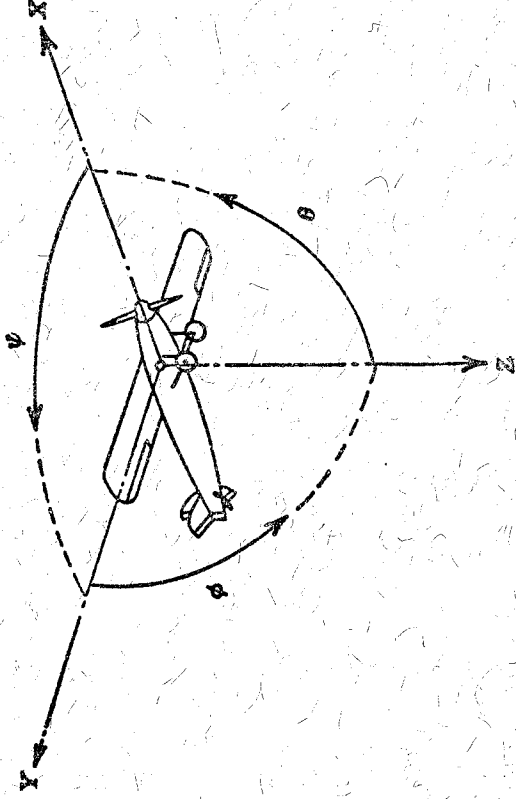


Figure 10.—Test of triangular airfoil in Langley model supersonic tunnel. Mach number, 1.75; Reynolds number, 1,600,000.



Positive directions of axes and angles (forces and moments) are shown by arrows

Axis		Force (parallel to axis) symbol		Moment about axis		Angle		Velocities	
Designation	Symbol	Designation	Symbol	Designation	Symbol	Designation	Symbol	Linear (component along axis)	Angular
Longitudinal	X	Rolling	L	Y → Z	Roll	φ	u	p	
Lateral	Y	Pitching	M	Z → X	Pitch	θ	v	q	
Normal	Z	Yawing	N	X → Y	Yaw	ψ	w	r	

Absolute coefficients of moment

$$C_l = \frac{L}{q b S} \quad C_m = \frac{M}{q c S} \quad C_n = \frac{N}{q b S} \quad (\text{yawing})$$

Angle of set of control surface (relative to neutral position), δ . (Indicate surface by proper subscript.)

4. PROPELLER SYMBOLS

D	Diameter	P	Power, absolute coefficient $C_P = \frac{P}{\rho n^3 D^5}$
p	Geometric pitch	C_s	Speed-power coefficient $= \sqrt{\frac{\rho V^5}{P n^2}}$
p/D	Pitch ratio	η	Efficiency
V_i	Inflow velocity	n	Revolutions per second, rps
V_s	Slipstream velocity	Φ	Effective helix angle $= \tan^{-1} \left(\frac{V}{2\pi r n} \right)$
T	Thrust, absolute coefficient $C_T = \frac{T}{\rho n^2 D^4}$		
Q	Torque, absolute coefficient $C_Q = \frac{Q}{\rho n^2 D^5}$		

5. NUMERICAL RELATIONS

1 hp	= 76.04 kg-m/s = 550 ft-lb/sec
1 metric horsepower	= 0.9863 hp
1 mph	= 0.4470 mps
1 mps	= 2.2369 mph
1 lb	= 0.4536 kg
1 kg	= 2.2046 lb
1 m	= 1,609.35 m = 5,280 ft
1 m	= 3.2808 ft